Journal of Naval Science and Engineering
2011, Vol.7, No.2, pp. 11-29

NUMERICAL MODELLING OF UNDERWATER WELDING

Yasar Vehbi ISIKLAR[1], Ibrahim GIRGIN[2*]

[1]Turkish Naval Forces Command, Technics Department
Ankara,Turkiye
*[*2]Turkish Naval Academy Mechanical Engineering Department*
Tuzla, Istanbul,Turkiye
yvisiklar@yahoo.com, igirgin@dho.edu.tr

Abstract

In this study, a numerical method has been developed for modelling underwater welding. The geometry used in the study is a three-dimensional thick rectangular plate. Transient heat conduction in the plate has been calculated numerically including a point heat source simulating the arc and convective, radiative and boiling surface boundary conditions. Finite volume method has been used as the numerical scheme. A variable mesh size centered around the moving heat source has been used in the calculations. The validity of the results was checked by comparison with some solutions in the literature.

SU ALTI KAYNAĞININ SAYISAL MODELLEMESİ

Özetçe

Bu çalışmada, su altı kaynağının modellenmesi için sayısal bir yöntem geliştirilmiştir. Çalışmada kullanılan geometri üç boyutlu kalın bir plakadır. Plaka içerisinde zamana bağlı ısı iletimi kaynak elektrodunu simüle eden noktasal bir ısı kaynağı ve taşınım, ışınım ve kaynama sınır koşullarını kullanarak sayısal olarak hesaplanmıştır. Sayısal yöntem olarak sonlu hacim yöntemi kullanılmıştır. Hesaplarda hareketli ısı kaynağının etrafında değişken aralıkta bir grid yapısı kullanılmış ve sonuçların geçerliliği literatürdeki bazı çözümlerle karşılaştırılarak kontrol edilmiştir. .

Keywords : *Underwater Wet Welding, Finite Volume Method.*
Anahtar Kelimeler : *Sualtı Islak Kaynağı, Sonlu Hacim Yöntemi.*

1. INTRODUCTION

To improve the quality of the underwater welding and to accomplish a reliable, permanent underwater wet welding capability has a great importance in today's industrial facilities. With the development of underwater wet welding techniques, the time and the money required for permanent and temporary repairs of ships and other underwater structures can be minimized. Currently, underwater wet welding is used for the temporary repair needs. Because of their poor quality compared to surface (air) welds (they obtain 80% of the tensile strength and 50% ductility of the surface welds [1].), they must be replaced as soon as possible. Therefore, to develop a more efficient wet welding technique, a numerical model simulation is necessary.

In the present study, a numerical model has been developed for transient, three-dimensional conduction heat transfer in underwater welding process on a thick rectangular plate. The numerical scheme was based on finite volume model, including convection, radiation and boiling surface thermal boundary conditions. The different regimes of boiling were accounted for on the surface. A variable mesh size centered around an arc source moving at constant speed was used to determine temperature variations inside and around the weld pool. The weld pool region itself has been modeled as a solid region of thermal conductivity higher than the surrounding unmelted solid region. The input data from the previous studies based on different methods were used to check the accuracy and the validity of the numerical method.

2. BACKGROUND

2.1 Previous Studies

Rosenthal did the most important early work on the theory of the effect of moving sources of heat in the late of 1930s. He studied the fundamentals of this theory and derived equations for two-dimensional and three-dimensional heat conduction in a solid when a moving source is in use [2]. The assumptions used by Rosenthal were: Point heat source, No melting, constant thermal

properties, no heat loss from the workpiece surface, infinitely wide workpiece.

Recently, numerical analysis, methods and computer programs have been commonly used to develop the previous assumptions. In 1965, The Battelle Institute Geneva Laboratory in Switzerland conducted a computer-aided study about analyzing of heat flow in weldments. In 1970, M.I.T. researchers studied heat flow during underwater welding [3]. Oreper and Szekeley examined stationary, axisymmetric TIC (tungsten-inert-gas) welding process with a moving boundary by using finite difference method [4]. Kou and Wang performed computational studies of the GTA welding process. They presented a computer simulation of three-dimensional convection for an arc source moving at constant speed [5]. Correa and Sundell studied axisymmetric stationary arc source by using different grid sizes for computation of flow and electromagnetic fields [6]. Saedi and Unkel developed a thermal-fluid model of the weld pool. Their model was based on the stationary arc [7]. Zacharia et al. made three-dimensional calculations on the effects of the heat source in the stationary GTAW process [8]. Ule, Joshi and Sedy determined three-dimensional transient temperature variations in the GTAW process by using the explicit finite difference method. They used different mesh sizes and temperature dependent thermal properties. They also considered convective and radiative surface thermal conditions during calculations [9]. Kanouff and Greif studied the unsteady development of an axisymmetric arc weld pool in GTAW process. They used moving grids to follow the phase change boundary and considered the effects of Marangoni, Lorentz and buoyancy forces in the calculations [10]. Joshi, Dana, Schupp and Espinosa developed a three-dimensional numerical model to describe the flow circulation phenomena in aluminum weld pools under non-axisymmetric Lorentz force field [11,12].

2.2 Finite Volume Method

The finite volume method is one of the simple and well-established Computational Fluid Dynamics (CFD) techniques that were originally developed

as a special finite difference method. The stages of the numerical algorithm in this method are as follows [13]:

1. .Formal integration of the governing equations of fluid flow over all the finite control volumes of the solution domain.
2. Discretisation involves the substitution of a variety of finite difference type approximations for the terms in the integrated equation representing flow process such as convection, diffusion and sources. This converts the integral equations into a system of algebraic equations.
3. Solution of the algebraic equations by an iterative method.

To understand the finite volume method better an illustrative example can be given for one-dimensional steady state heat conduction situation.

The governing equation for one-dimensional steady state heat conduction is

$$\frac{d}{dx}\left(k\frac{dT}{dx}\right)+S=0 \qquad (1)$$

where k is thermal conductivity, T is temperature, and S is the rate of heat generation per unit volume. The domain is divided into small and nonoverlapping control volumes. (Figure 1)

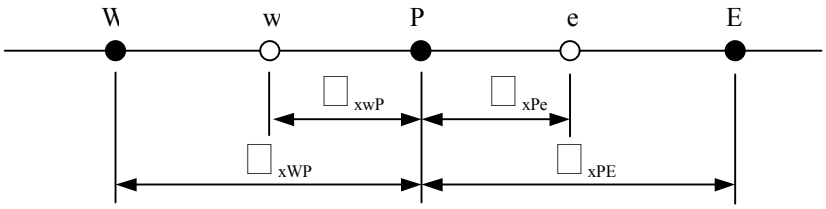

Figure 1 : The discretisation of the geometry.

The equation can be discretised as:

$$\left(k\frac{dT}{dx}\right)_e - \left(k\frac{dT}{dx}\right)_w + \bar{S}\Delta x = 0$$

$$k_e\left(\frac{T_E - T_P}{\delta_{xPE}}\right) - k_w\left(\frac{T_P - T_W}{\delta_{xWP}}\right) + \bar{S}\Delta x = 0$$

$$a_P T_P = a_E T_E + a_W T_W + b$$

where

$$a_E = \frac{k_E}{\delta_{xPE}},\ a_W = \frac{k_W}{\delta_{xWP}},\ a_P = a_E + a_W, \text{ and } b = \bar{S}\Delta x.$$

3. GOVERNING EQUATION AND BOUNDARY CONDITIONS

3.1 Governing Equation

The problem is governed by the equation:

$$\rho c\frac{\partial T}{\partial t} = \frac{\partial}{\partial x}\left(k\frac{\partial T}{\partial x}\right) + \frac{\partial}{\partial y}\left(k\frac{\partial T}{\partial y}\right) + \frac{\partial}{\partial z}\left(k\frac{\partial T}{\partial z}\right) \qquad (2)$$

The geometry of the problem is seen in Figure 1.

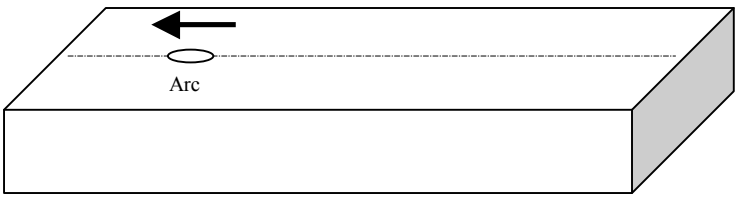

Figure 1: The geometry of the problem.

3.2 Boundary Conditions

3.2.1 Top Face

Boundary condition for the top face including convective and radiative heat loss and heat fluxes:

$$-k\frac{dT}{dx} = h\left(T_{wall} - T_{\infty}\right) + q^{"} + \sigma\varepsilon\left(T_{wall}^{4} - T_{surr}^{4}\right) \tag{3}$$

where

$$q_{top}^{"} = q_{source}^{"} + q_{boiling}^{"}$$

$q_{source}^{"}$ is arc source heat flux, and $q_{boiling}^{"}$ is boiling heat flux.

3.2.2 Other Faces

The boundary conditions for the other faces are the same of top face without radiation term:

$$-k\frac{dT}{dx} = h\left(T_{wall} - T_{\infty}\right) + q^{"}$$

3.2.3 Simulating the Arc

It is assumed that the arc has a Gaussian distribution on the top face of the workpiece. The equation for the arc is:

$$Q = q_o \int_0^{\infty} e^{-\frac{d}{r_o^2}r^2}\, 2\pi r dr \tag{4}$$

where Q is the total heat input into the workpiece, r_o is the radius of the heat input distribution, d is the exponential factor, and q_o is the volumetric energy

generation rate, $q_o = \frac{Qd}{\pi r_o^2}$.

3.2.4 Boiling Heat Transfer

Boiling modes that were used in the analysis are as follows: (where $\Delta T_e = T_s - T_{sat}$, ΔT_e is the difference between surface temperature and saturation temperature)

3.2.4.1 Free Convection Regime ($\Delta T_e \le 5^o C$)

Natural convection effects determine the heat transfer mode between surface temperature and the surrounding fluid. Recommended correlations for the top heated surface are: [14]

$$\overline{Nu}_L = 0.54 Ra_L^{1/4} \qquad (10^4 \le Ra_L \le 10^7) \tag{5.a}$$

$$\overline{Nu}_L = 0.15 Ra_L^{1/3} \qquad (10^7 \le Ra_L \le 10^{11}) \tag{5.b}$$

where the Rayleigh number is,

$$Ra_L = \frac{g\beta(T_s - T_\infty)L^3}{\upsilon\alpha} \tag{5.c}$$

g is the gravitational acceleration, β is thermal expansion coefficient, υ is kinematic viscosity, α is thermal diffusivity, L is characteristic length, L=surface area/perimeter of plate, k is thermal conductivity and

$$\bar{h} = \frac{\overline{Nu}_L k}{L}$$

Heat flux is $q'' = \bar{h}(T_s - T_\infty)$.

3.2.4.2 Nucleate Boiling Regime ($5^o C < \Delta T_e \leq 30^o C$)

The correlation developed by Rohsenow was used: [14,15,16]

$$q_s^s = \mu_l h_{fg} \left[\frac{g(\rho_l - \rho_v)}{\sigma} \right]^{1/2} \left(\frac{c_{p,l} \Delta T_e}{c_{s,f} h_{fg} \, \mathrm{Pr}_l^n} \right)^3 \tag{6.a}$$

$$\tau = \frac{\pi}{3} \sqrt{2\pi} \left[\frac{\sigma}{g(\rho_l - \rho_v)} \right]^{1/2} \left[\frac{\rho_v^2}{\sigma g(\rho_l - \rho_v)} \right]^{1/4} \tag{6.b}$$

$$q'' = q_s'' \left\{ 1 + \left[\frac{2k_l (T_{sat} - T_{liquid})}{\sqrt{\pi \alpha_l \tau}} \right] \frac{24}{\pi h_{fg} \rho_v} \left[\frac{\rho_v^2}{\sigma g(\rho_l - \rho_v)} \right]^{1/4} \right\} \tag{6.c}$$

where μ_l is viscosity of the liquid, h_{fg} is latent heat of vaporization, ρ_l is density of the saturated liquid, ρ_v is density of the saturated vapor, σ is surface tension of the liquid-to-vapor interface, $c_{p,l}$ is specific heat of saturated liquid, Pr_l is Prandtl number of the saturated liquid, n = 1.0 for water, 1.7 for other fluids, $C_{s,f}$ is the empirical constant that depends on the nature of the heating surface fluid combination and whose numerical value varies from system to system.

3.2.4.3 Transition Boiling Regime ($30^o C < \Delta T_e \leq 120^o C$)

For the transition-boiling regime, the heat flux is between the maximum and minimum heat fluxes: [14,15]

$$q''_{\max} = 0.149 h_{fg} \rho_v \left[\frac{\sigma g(\rho_l - \rho_v)}{\rho_v^2} \right]^{1/4} \tag{7.a}$$

$$q''_{\min} = 0.09 h_{fg} \rho_v \left[\frac{\sigma g (\rho_l - \rho_v)}{(\rho_l + \rho_v)^2} \right]^{1/4} \tag{7.b}$$

By assuming logarithmically linear heat flux distribution, the heat flux at a point in transition regime is:

$$\log(q'') = \frac{\log\left(\frac{q''_{\max}}{q''_{\min}}\right)}{\log\left(\frac{30}{120}\right)} \log\left(\frac{\Delta T_e}{120}\right) + \log\left(q''_{\min}\right) \tag{7.c}$$

and $q'' = 10^{\log(q'')}$

3.2.4.4 Film Boiling Regime ($\Delta T_e > 120^o C$)

Westwater and Breen recommended the following corelation for film boiling regime: [15]

$$\bar{h}_c = 0.59 \left\{ \frac{g(\rho_l - \rho_v)\rho_v k_v^3 \left[h_{fg} + 0.68 c_{pv} \Delta T_e \right]}{\lambda \mu_v \Delta T_e} \right\}^{1/4} \tag{8.a}$$

where μ_v is viscosity of the vapor, k_v is thermal conductivity of vapor, and c_{pv} is specific heat of saturated vapor, $\lambda = 2\pi \left[\frac{\sigma}{g(\rho_l - \rho_v)} \right]^{1/2}$

Bromley suggested combining convection and radiation heat transfer coefficients: [15]

$$\bar{h}_r = \sigma \varepsilon_s \left(\frac{T_s^4 - T_{sat}^4}{T_s - T_{sat}} \right) \tag{8.b}$$

$$\bar{h}_{total} = \bar{h}_c + 0.75 \bar{h}_r \tag{8.c}$$

where ε_s is surface emissivity, T_s is absolute surface temperature.

Heat flux from the surface is $q'' = \bar{h}_{total} \Delta T_e$.

4. RESULTS AND DISCUSSION

Validity of the model were compared to some results in the literature. A variable sized and moving numerical mesh was used in such a way that the arc was always positioned at the center of the mesh where the spacing is the finest. The goal is to be able to resolve the large temperature gradient features around the arc. The weld pool region was also modeled as a solid region but with a thermal conductivity higher than the surrounding region to simulate the effects of weld pool convection. The discontinuity in the thermal conductivity boundaries was handled using the standard technique of employing harmonic averaging at the boundary. Since the coefficients of the system of equations depend on the temperature, an iterative solution technique was used to achieve convergence in such a way that the maximum temperature difference between two consecutive iterations at any grid point was no more than $0.1^{o}C$ .The numerical solution method was used to examine different cases in freshwater for a 40-mm-thick 70 x 90 mm workpiece with a moving heat source in the positive y-direction.

4.1 Case 1

The validity of the numerical model was compared to Rosenthal's solution. The calculations were made up to 3.6 seconds. The numerical results show excellent agreement with the analytical results of Rosenthal (Figure 2 and Figure 3). The input data used in computations for Case 1 is shown in Table 1.

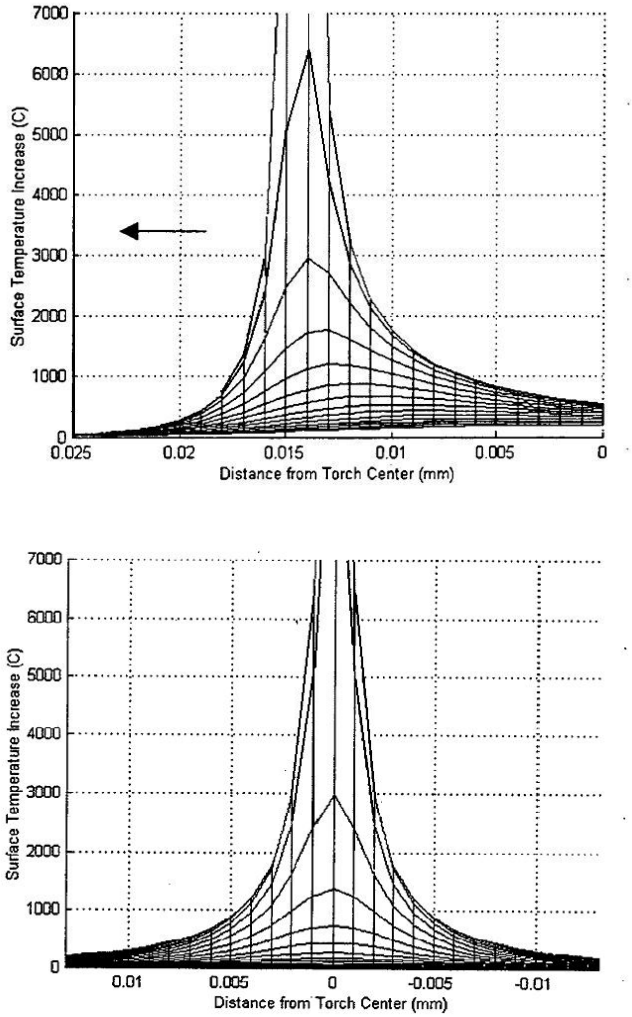

Figure 2: Rosenthal's point heat source solution: (a) Profile; (b) Front-view.

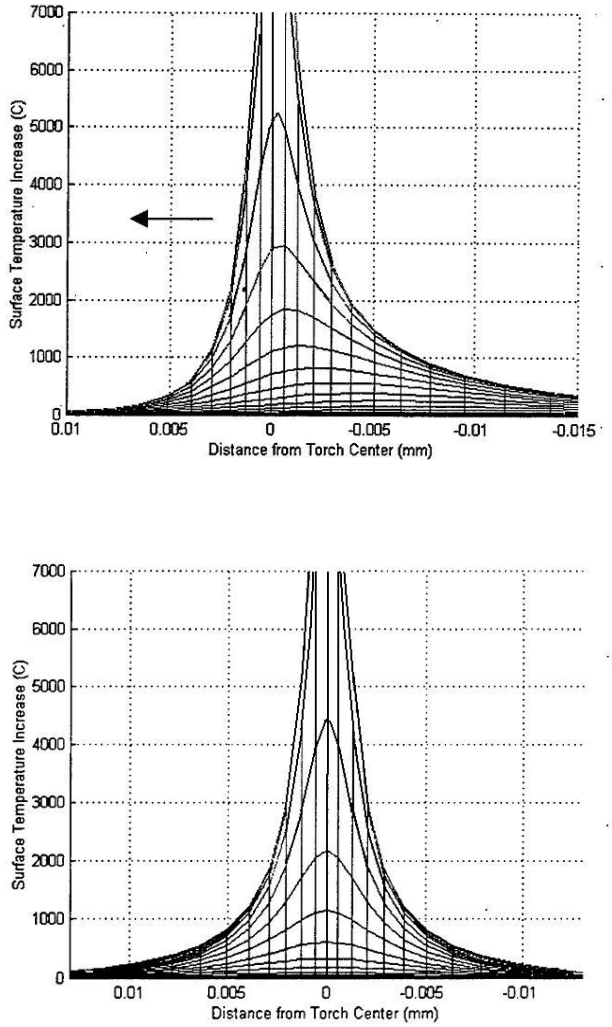

Figure 3: The numerical model point heat source solution: (a) Profile; (b) Front-view

Workpiece :	*Length - 70 mm, Width – 90 mm*
Water temperature:	T=*27^o C*
Power input into workpiece :	Q=*2544 W*
Arc torch speed :	V_y = *4 mm/s*
Radius of heat input distribution :	r_o = *4.5 mm*
Thermal conductivity :	k = *53 W/m K*
Density of steel :	ρ = *7854 kg\m^3*
Specific heat of steel :	*Cp = 509.3 J/kgK*

Table 1 : The input data used in Case 1.

4.1 Case 2

In this case, the surface thermal boundary conditions of boiling heat transfer were included. Other relevant data is given in Table 2.

Workpiece :	*Length - 70 mm, Width – 90 m, Thickness – 40 mm*
Water temperature:	*T=27 ^{o}C*
Saturation temperature:	*T=100 ^{o}C*
Water depth :	*l=0 m*
Total pressure:	*P=101.325 kPa*
Power input into workpiece :	*Q=2544 W*
Arc torch speed :	V_y = *4 mm/s*
Radius of heat input distribution :	r_o = *4.5 mm*
Thermal conductivity : W/m.K	*53 - 0.04 (T-300)* *300 < T(K) < 1000*
	25 + 6.25 x 10^{-3} (T-1000) *1000 < T(K) < 1800*
	125 *T(K) > 1800*
Emissivity:	ε =0.82

Table 2 : The input data used in Case 2.

The top surface temperature values at 0.5 seconds can be seen in Figure 4 and Figure 5. At t=0.5 sec, the temperature distribution is almost symmetric about the position of the arc.The temperature distribution around

the arc center is above the melting temperature of the workpiece(Tm= 1800K)

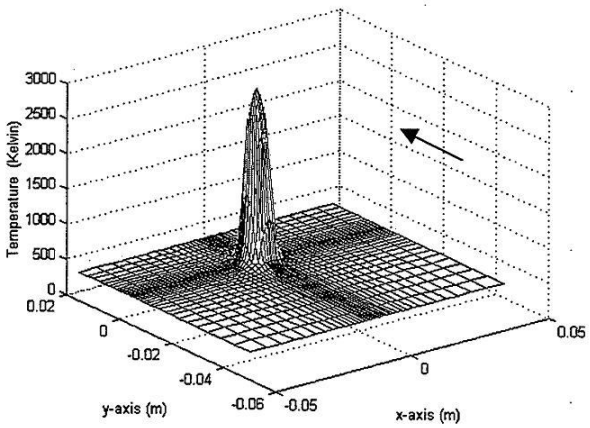

Figure 4: Top surface t=0.5 sec

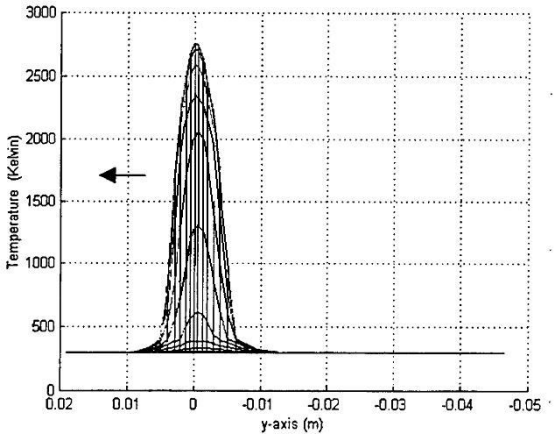

Figure 5: Top surface (profile) t=0.5 sec

To see the depth of the weld pool penetration, the melting temperature contours were plotted for different surfaces (Figure 6) and the weld pool depth was shown through the melting temperature points by using a curve-fit (Figure 7).Because of the brief reaction time, the arc heat input penetration to the workpiece is limited and a well-formed weld pool cannot be seen. [9]

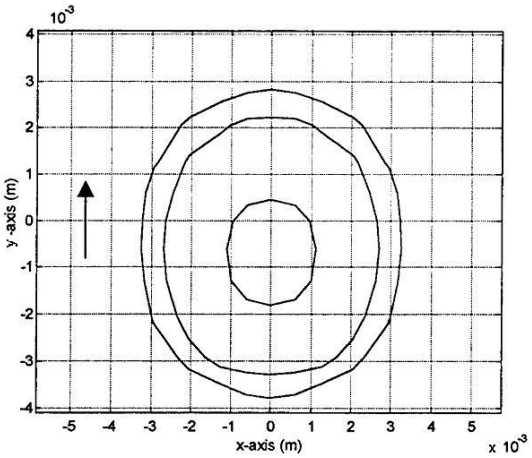

Figure 6: The weld pool surface characteristics by the T=1800 K contours t=0.5 sec

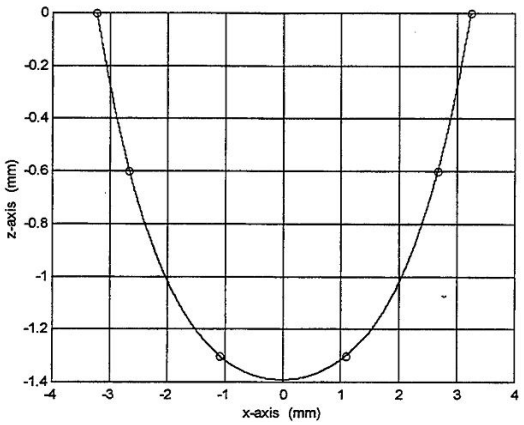

Figure 7: The weld pool (front-view) t=0.5 sec

At t= 4.5 sec., the temperature distribution on the plate is seen in Figure 8 and Figure 9. The melting temperature contours are still seen till the fourth surface from the top (Figure 10). But, the weld pool depth reached to 3 mm with a width of 8 mm (Figure 11). These results show a good agreement with the data from Ref.9.

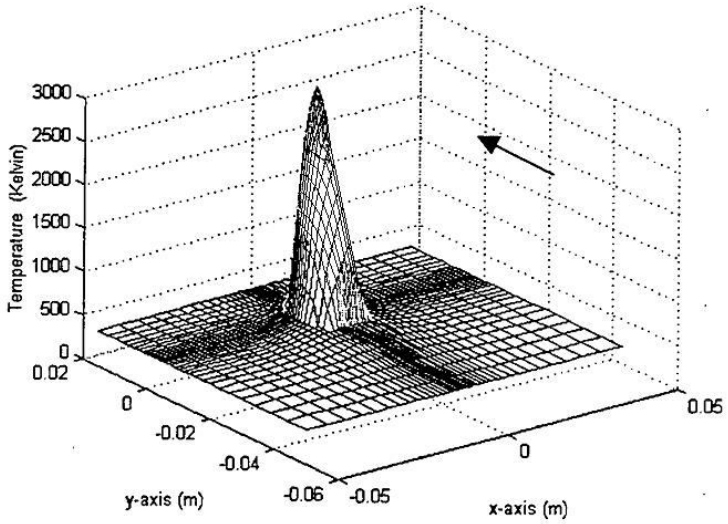

Figure 8: Top surface t=4.5 sec

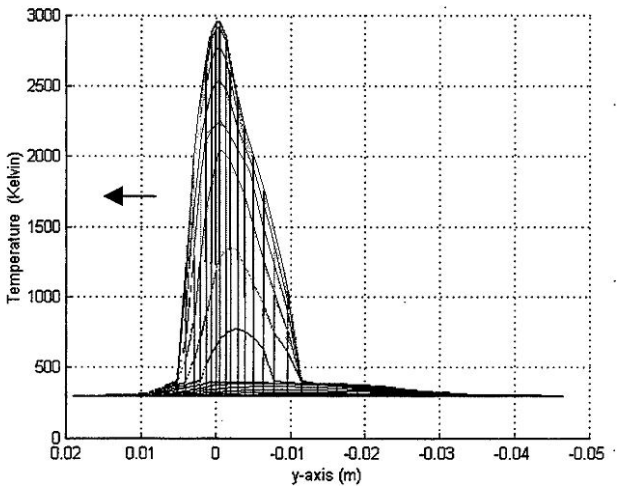

Figure 9: Top surface (profile) t=4.5 sec

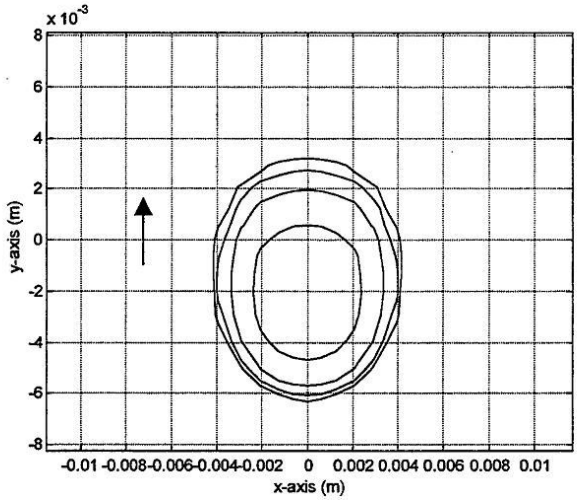

Figure 10: The weld pool surface characteristics by the T=1800 K contours t=4.5 sec

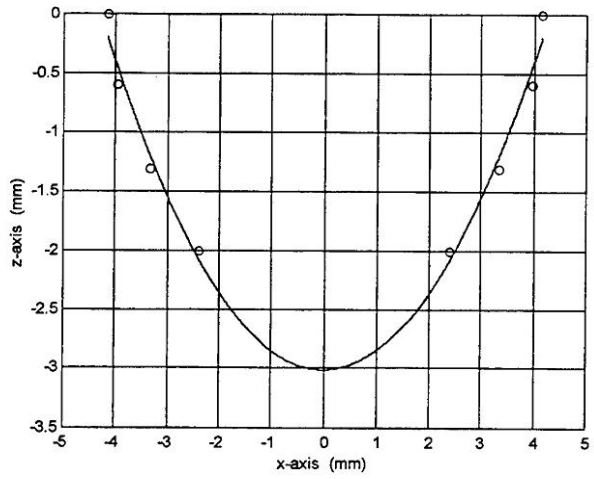

Figure 11: The weld pool (front-view) t=4.5sec

5. CONCLUSION

Compared, to experimental methods, numerical solution techniques are very fast, effective and economical alternatives. Therefore, it was developed a general numerical model for transient, three-dimensional conduction heat transfer phenomena in underwater welding process on a thick rectangular plate. Computations were presented for different cases. Comparisons of current predictions with results in the literature showed good agreement and validated the model. If the material, environment and the arc source properties are known, this program can be applied to the different types of metals under the wet welding process.

The numerical model gave important temperature-time data in the critical heat affected zone which in turn determines material structure.The model also helped to make prediction of size of weld pool and its evolution with time.

REFERENCES

[1] "Underwater Cutting and Welding," U.S. Navy Technical Manual, U.S.N. Supervisor of Diving, Naval Ship Systems Command.

[2] Rosenthal, D.," The Theory of Moving Sources of Heat and Its Application to Metal Treatments," Transactions of TheAS.M.E. Vol. 68, pp. 849-866, November 1946.

[3] Masubuchi, K., Analysis of Welded Structures, 1st Ed. London, Pergamon Press, 1980.

[4] Oreper, G.M. and Szekely, J., "Heat and Fluid-Flow Phenomena in Weld Pools, "Journal of Fluid Mechanics, Vol.147, pp. 53-79,1984.

[5] Kou, S. and Wang, Y.H., "Computer Simulation of Convection in Moving Arc Weld Pools," Metallurgical Transactions A, Vol. 17A, pp. 2271-2277, December 1986.

[6] Correa, S.M. and Sundeil, R.E., "A Computational and Experiment Study of The Fluid Flow in Weld Pools," S. Kou and R. Mehrabian. Eds., Modeling and Control of Casting and Welding Processes, Metallurgical Society, pp. 211-227, Warrendale, PA,1986.

[7] Saedi, H.R. and Unkel, W., " Thermal-Fluid Model for Weld Pool Geometry Dynamics," Journal of Dynamic Systems, Measurement and Control, Vol. III, pp. 268-276, June 1989.

[8] Zacharia, T., Eraslan, A.H., Aidun, D.K. and David, S.A., " Three-Dimensional Transient Model for Arc Welding Process," Metallurgical Transactions, Vol. 20B, pp. 645-659, October 1989.

[9] Ule, R.L., Y. Joshi and E.B. Sedy, "A New Technique for Three-Dimensional Transient Heat Transfer Computations of Autogenous Arc Welding," Metallurgical Transactions B, Vol.21B, pp.1033-1047,Dec. 1990.

[10] Kanouff, M. and Greif, R., " The Unsteady Development of a GTA Weld Pool,"Int. Journal of Heat and Mass Transfer, Vol. 35, pp. 967-969.

[11] Joshi, Y., Dutta, P., Schupp, P.E., Espinosa, D., "Nonaxisymmetric Convection in Stationary Gas Tungsten Arc Weld Pools," Journal of Heat Transfer, Vol. 119, pp. 164-172, February 1997.

[12] Espinosa, D.C., Master's Thesis, Naval Postgraduate School, Monterey, CA, 1991.

[13] Versteeg, H.K. and Malalasekera, W., An Introduction to Computational Fluid Dynamics The Finite Volume Method, Longman Group Ltd., 1995.

[14] Incropera, F.P. and De Witt, D.P., Introduction to Heat Transfer, 3rd Ed., John Wiley& Sons, 1996.

[15] Kreith, F. and Bohn, M.S., Principles of Heat Transfer, 5th Ed., West Publishing Company, St. Paul, MN, 1993.

[16] Rohsenow, W.M. and Choi, H., Heat, Mass and Momentum Transfer, Prentice-Hall, Inc., New Jersey, 1961.